[7] Brown, K. R. and Johnson, G. W., "Real-Time Optimal Guidance," *IEEE Transactions on Automatic Control*, Vol. AC-12, No. 5, 1967, pp. 501–506.

[8] Brown, K. R., Harold, E. F., and Johnson, G. W., "Rapid Optimization of Multiple-Burn Rocket Flights," NASA CR-1430, Sept. 1969.

[9] Bryson, A. E. and Ho, Y. C., *Applied Optimal Control*, Blaisdell Publishing Co., Waltham, Mass., 1969.

[10] Kelley, H. J., "A Second Variation Test for Singular Extremals," *AIAA Journal*, Vol. 2, No. 8, 1964, pp. 1380–1382.

[11] Kelley, H. J., Kopp, R. E., and Moyer, H. G., "Singular Extremals," *Topics in Optimization*, edited by G. Leitman, Academic Press, 1967.

[12] McDanell, J. P. and Powers, W. F., "Necessary Conditions for the Joining of Optimal Singular and Nonsingular Subarcs," *SIAM Journal on Control*, Vol. 9, No. 2, May 1971, pp. 161–173.

[13] Powers, W. F. and McDanell, J. P., "Switching Conditions and a Synthesis Technique for the Singular Saturn Guidance Problem," AIAA Paper 70-965, Santa Barbara, Calif., 1970.

OCTOBER 1971 J. SPACECRAFT VOL. 8, NO. 10

Dynamically Unbalanced Dual-Spin Space Stations with Rigid or Low-Coupling Interconnections

RICHARD A. WENGLARZ*
Bellcomm Inc., Washington, D.C.

Effects of dynamic unbalances are determined for an axially symmetrical, dual-spin space station consisting of a rotating artificial gravity section and a controlled, despun zero gravity section. Configurations with either a rigid interconnection or a low-coupling flexible interconnection between sections are considered. Amplitudes of motion and control system requirements are compared for these configurations. Both configurations are found to experience coning motions. For large space stations with rigid interconnection, control moment gyros (CMGs) are found impractical for reducing coning motions to within allowable limits for many experiments and special systems such as active mass balancing are necessary. However, for a flexible interconnection, coning motions of the despun section are substantially reduced and CMGs could be utilized to reduce motions to acceptable levels.

Introduction

SEVERAL studies[1–3] have been conducted in recent years on the attitude motion of dual-spin spacecraft consisting of two bodies with relative motion restricted to rotations about a common axis fixed in both. However, it has been proposed[4] that a low-coupling interconnection which also permits relative rotations of the bodies about directions normal to that axis may offer advantages over the rigid interconnection. Reference 4 states that a low-coupling interconnection designed to transmit only low-levels of torque normal to the common axis could attenuate the effects of mass unbalances of the spinning section on the motion of the despun section.

A recent study[5] has determined that such isolation does occur and that dissipation in a flexible interconnection is an effective means of attenuating nutation. However, that study considers a passive system except for a constant speed motor driving the spinning section at a fixed relative rate. Following is an analysis of the effects of dynamic mass unbalances on attitude motion and stability for dual-spin satellites that are actively controlled by control moment gyros (CMGs) and have either a rigid interconnection or a low-coupling interconnection. A comparison is then given for amplitudes of motion and CMG requirements for the two interconnections and the results are applied to a large space base.

Received March 16, 1971; revision received June 24, 1971.
Index category: Spacecraft Attitude Dynamics and Control.

* Member of Technical Staff, Rotational Dynamics and Attitude Control Group.

System Description

The space station dynamical model to be considered is shown in Fig. 1 and consists of two sections attached by a massless gimbal arrangement. The satellite is stabilized by CMGs providing three axis control on one of the sections. The other section is assumed driven at a constant rate about a line which is not a principal axis of inertia for that body.

System details and terminology are given as follows: The spinning section is termed body B and the other section is termed body A. Both are axially symmetrical with principal moments of inertia for their mass centers denoted by B_3 and A_3, respectively, in the directions of the symmetry axes, and B_1 and A_1, respectively, in directions normal to the symmetry axes. For body B, the mass is designated M_B, the mass center is designated B^*, and a right-handed, mutually orthogonal set of unit vectors parallel to principal axes of B at B^* is designated by $\mathbf{b}_1$, $\mathbf{b}_2$, $\mathbf{b}_3$. Similar quantities for body A are mass M_A, mass center A^*, and unit vectors $\mathbf{a}_1$, $\mathbf{a}_2$, $\mathbf{a}_3$, parallel to principal axes at A^*.

An inertially fixed set of unit vectors $\mathbf{a}_{10}$, $\mathbf{a}_{20}$, $\mathbf{a}_{30}$, is defined by the initial orientation of $\mathbf{a}_1$, $\mathbf{a}_2$, $\mathbf{a}_3$ at time $t = 0$. The orientation of $\mathbf{a}_1$, $\mathbf{a}_2$, $\mathbf{a}_3$ (and consequently A) at some subsequent time t is described with respect to $\mathbf{a}_{10}$, $\mathbf{a}_{20}$, $\mathbf{a}_{30}$, by a 1,2,3 sequence of three axis Euler angles ϕ_1, ϕ_2, ϕ_3. Also, the CMG control torque on A is assumed related to ϕ_1, ϕ_2, ϕ_3, by

$$\mathbf{T}^A = -[(K_0\phi_1 + K_1\dot{\phi}_1)\mathbf{a}_1 + (K_0\phi_2 + K_1\dot{\phi}_2)\mathbf{a}_2 + (K_{03}\phi_3 + K_{13}\dot{\phi}_3)\mathbf{a}_3] \quad (1)$$

where K_0, K_{03}, K_1, K_{13} are measures of the level of attitude control.

Body B is driven at a constant rate ω about a drive axis which is slightly misaligned from the principal axis in the direction of $\mathbf{b}_3$. Let $\mathbf{b}_1'$, $\mathbf{b}_2'$, $\mathbf{b}_3'$ be a right-handed set of mutually orthogonal unit vectors fixed in B with $\mathbf{b}_3'$ in the direction of the drive axis and let the transfer relations between $\mathbf{b}_i$ and $\mathbf{b}_j'$ be given by

$$\mathbf{b}_i = \sum_{j=1}^{3} b_{ji}\mathbf{b}_j' \tag{2}$$

The drive axis of B intersects B^* and point 0 which is the common intersection of the symmetry axis of A and the axes of the gimbal connecting A and B. A^* and B^* are located at distances l_A and l_B, respectively, from 0. Rotations θ_1 about gimbal axis G_1 and θ_2 about gimbal axis G_2 describe the orientation of the drive axis of B with respect to $\mathbf{a}_1$, $\mathbf{a}_2$, $\mathbf{a}_3$ as shown in Fig. 1. Unit vectors $\mathbf{c}_1$, $\mathbf{c}_2$, $\mathbf{c}_3$ are designated such that $\mathbf{c}_3$ is parallel to the drive axis, $\mathbf{c}_2$ is parallel to G_2, and $\mathbf{c}_1$ completes the mutually orthogonal right-handed set. Motion of A relative to B is resisted by gimbal axes torque ${}^G\mathbf{T}^A$ on A with components ${}^G\mathbf{T}_i{}^A$ along G_i given by

$$G_{T_i}A = C_0\theta_i + C_1\dot{\theta}_i \qquad i = 1,2 \tag{3}$$

Coefficients C_0 and C_1 are associated with gimbal stiffness and dissipation, respectively.

Equations of Motion

Gravity gradient and other environmental torques will be neglected in the formulation of equations of motion because, for rotation rate ω much greater than orbital rate, their magnitudes are much smaller than the magnitude of torque associated with misalignment of the spin axis of B.

The three Euler angles ϕ_1, ϕ_2, ϕ_3, which describe the orientation of body A relative to inertially fixed axes, the two gimbal angles θ_1 and θ_2, and the prescribed rotation ωt of B about its spin axis provide a complete description of the satellite orientation. Euler's dynamical equations for rotational motions together with Newton's equations for translational motions of A and B may be written in terms of these variables. Reaction forces between A and B may be eliminated from the rotational equations of motion using the translational equations of motion. Linearization of the resulting equations about initial state $\phi_i = \theta_j = 0$, $i = 1,2,3$; $j = 1,2$, yields

$$\ddot{\phi}_1[B_1 + Bb_1 + Ml_B(l_A + l_B) + B(-b_2s2\omega t + b_3c2\omega t)] + \ddot{\phi}_2B(b_3s2\omega t + b_2c2\omega t) + 2\dot{\phi}_3Bb_{33}(b_{13}c\omega t - b_{23}s\omega t) + \ddot{\theta}_1[B_1 + Bb_1 + Ml_B{}^2 + B(-b_2s2\omega t + b_3c2\omega t)] + \ddot{\theta}_2B(b_3s2\omega t + b_2c2\omega t) - \dot{\phi}_1\omega B(b_3s2\omega t + b_2c2\omega t) + \dot{\phi}_2\omega[B_3 - Bb_1 + B(-b_2s2\omega t + b_3c2\omega t)] - 4\dot{\phi}_3\omega Bb_{33}(b_{23}c\omega t + b_{13}s\omega t) + \dot{\theta}_1[C_1 - \omega B(b_3s2\omega t + b_2c2\omega t)] + \dot{\theta}_2\omega[B_3 - Bb_1 + B(-b_2s2\omega t + b_3c2\omega t)] + \theta_1C_0 = 2\omega^2Bb_{33}(b_{23}c\omega t + b_{13}s\omega t) \tag{4}$$

$$\ddot{\phi}_1B(b_3s2\omega t + b_2c2\omega t) + \ddot{\phi}_2[B_1 + Bb_1 + Ml_B(l_A + l_B) + B(b_2s2\omega t - b_3c2\omega t)] + 2\dot{\phi}_3Bb_{33}(b_{23}c\omega t + b_{13}s\omega t) + \ddot{\theta}_1B(b_3s2\omega t + b_2c2\omega t) + \ddot{\theta}_2[B_1 + Bb_1 + Ml_B{}^2 + B(b_2s2\omega t - b_3c2\omega t)] - \dot{\phi}_1\omega[B_3 - Bb_1 + B(b_2s2\omega t - b_3c2\omega t)] + \dot{\phi}_2\omega B(b_3s2\omega t + b_2c2\omega t) + 4\dot{\phi}_3\omega Bb_{33}(b_{13}c\omega t - b_{23}s\omega t) - \dot{\theta}_1\omega[B_3 - Bb_1 + B(b_2s2\omega t - b_3c2\omega t)] + \dot{\theta}_2[C_1 + \omega B(b_3s2\omega t + b_2c2\omega t)] + \theta_2C_0 = -2\omega^2Bb_{33}(b_{13}c\omega t - b_{23}s\omega t) \tag{5}$$

$$2\ddot{\phi}_1Bb_{33}(b_{13}c\omega t - b_{23}s\omega t) + 2\ddot{\phi}_2Bb_{33}(b_{23}c\omega t + b_{13}s\omega t) + \ddot{\phi}_3(A_3 + B_3 - 2Bb_1) + 2\ddot{\theta}_1/Bb_{33}(b_{13}c\omega t - b_{23}s\omega t) + 2\ddot{\theta}_2Bb_{33}(b_{23}c\omega t + b_{13}s\omega t) + \dot{\phi}_3K_{13} + \phi_3K_{03} = 0 \tag{6}$$

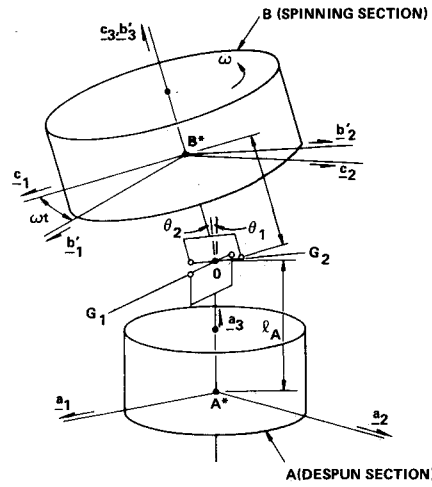

Fig. 1 Dual-spin spacecraft with flexible interconnection.

$$\ddot{\phi}_1[A_1 + Ml_A(l_A + l_B)] + \ddot{\theta}_1Ml_Al_B + \dot{\phi}_1K_1 + \phi_1K_0 - \dot{\theta}_1C_1 - \theta_1C_0 = 0 \tag{7}$$

$$\ddot{\phi}_2[A_1 + Ml_A(l_A + l_B)] + \ddot{\theta}_2Ml_Al_B + \dot{\phi}_2K_1 + \phi_2K_0 - \dot{\theta}_2C_1 - \theta_2C_0 = 0 \tag{8}$$

where $B = (B_3 - B_1)/2 \quad M = M_AM_B/(M_A + M_B)$

$$b_1 = b_{13}{}^2 + b_{23}{}^2 \quad b_2 = 2b_{13}b_{23} \quad b_3 = b_{13}{}^2 - b_{23}{}^2 \tag{9}$$

and

$$s2\omega t = \sin 2\omega t \quad c2\omega t = \cos 2\omega t$$

Although linearized, these equations involve periodic coefficients and standard techniques for a closed form solution are not available. However, they can be written in a standard matrix form that will be seen to have a stable steady-state periodic solution which may be represented through a method of successive approximations for small spin axis misalignments.

Now, establishment of a new independent variable, $\tau = \omega t$, so that $d(\ )/dt = \omega d(\ )/d\tau = \omega(\ )'$, the writing of Eqs. (4–8) in terms of τ, solution of these equations for ϕ_1'', ϕ_2'', ϕ_3'', θ_1'', θ_2'' and definition of a vector x with components x_i given by

$$\begin{aligned} x_i &= x_{i+5}' \qquad i = 1, \ldots, 5 \qquad x_{i+5} = \phi_1 \\ i &= 1,2,3 \qquad x_{j+8} = \theta_j \qquad j = 1,2 \end{aligned} \tag{10}$$

along with

$$\begin{aligned} n_{11} &= e_1k_1/\Delta \quad n_{12} = e_2a/\Delta \quad n_{13} = (ah_{12} + e_1h_{11})/\Delta \\ n_{14} &= e_1k_0/\Delta \quad n_{15} = (ah_{02} + e_1h_{01})/\Delta \\ n_{21} &= k_1/\Delta \quad n_{22} = e_2/\Delta \quad n_{23} = (h_{12} + h_{11})/\Delta \\ n_{24} &= k_0/\Delta \quad n_{25} = (h_{02} + h_{01})/\Delta \\ n_{31} &= k_{13} \quad n_{32} = k_{03} \quad \Delta = e_1 - a \end{aligned} \tag{11}$$

where

$$\begin{aligned} e_1 &= (B_1 + Ml_B{}^2)/J_2 \quad e_2 = B_3/J_2 \quad h_{12} = C_1/\omega J_2 \\ h_{02} &= C_0/\omega^2J_2 \quad a = Ml_Al_B/J_1 \quad k_1 = K_1/\omega J_1 \\ k_0 &= K_0/\omega^2J_1 \quad h_{11} = C_1/\omega J_1 \quad h_{01} = C_0/\omega^2J_1 \\ k_{13} &= K_{13}/\omega J_3 \quad k_{03} = K_{03}/\omega^2J_3 \end{aligned} \tag{12}$$

and

$$J_1 = A_1 + Ml_A(l_A + l_B) \quad J_2 = B_1 + Ml_B(l_A + l_B) \quad J_3 = A_3 + B_3 \quad d = B/J_2 \tag{13}$$

yields equations of motion in a standard matrix form,

$$x' = [D + F(\tau,\mu)]x + g(\tau,\mu) = f(\tau,x,\mu) \tag{14}$$

where μ is a two-dimensional vector,

$$\mu = \begin{bmatrix} b_{13} \\ b_{23} \end{bmatrix} \tag{15}$$

Constant matrix D and column vector g are given by

$$D = \left[\begin{array}{ccccc|ccccc} -n_{11} & n_{12} & 0 & n_{13} & n_{12} & -n_{14} & 0 & 0 & n_{15} & 0 \\ -n_{12} & -n_{11} & 0 & -n_{12} & n_{13} & 0 & -n_{14} & 0 & 0 & n_{15} \\ 0 & 0 & -n_{31} & 0 & 0 & 0 & 0 & -n_{32} & 0 & 0 \\ n_{21} & -n_{22} & 0 & -n_{23} & -n_{22} & n_{24} & 0 & 0 & -n_{25} & 0 \\ n_{22} & n_{21} & 0 & n_{22} & -n_{23} & 0 & n_{24} & 0 & 0 & -n_{25} \\ \hline 1 & & & & & & & & & \\ & 1 & & & & & & & & \\ & & 1 & & & & & & & \\ & & & 1 & & & & & & \\ & & & & 1 & & & & & \end{array}\right] \tag{16}$$

$$g = [-ag_1 - ag_2 \quad 0 \quad g_1 \quad g_2 \quad 0 \quad 0 \quad 0 \quad 0 \quad 0]^T$$

where

$$\begin{aligned} g_1 &= 2d_1(1 - b_{13}^2 - b_{23}^2)^{1/2}(b_{23}c\tau + b_{13}s\tau) \\ g_2 &= 2d_1(1 - b_{13}^2 - b_{23}^2)^{1/2}(b_{23}s\tau - b_{13}c\tau) \end{aligned} \tag{17}$$

in which $d_1 = d/[\Delta +$ terms of order 2 and higher in $b_{13}, b_{23}]$. The matrix $F(\tau,\mu)$ is periodic in τ with period 2π with all elements proportional to first and higher powers in b_{13} and b_{23}. Consequently, for $b_{13} = b_{23} = 0$ then $\mu = 0$ and both $F(\tau, 0)$ and $g(\tau,0)$ are zero.†

As discussed in Appendix A, Coddington and Levinson[6] have established a method of successive approximations for finding periodic solutions to systems of equations with a small real constant vector μ provided certain conditions are satisfied. These conditions applied to the problem at hand are: 1) $x' = f(\tau,x,0) = Dx$ has no periodic solution of period 2π other than the trivial solution $x = 0$, 2) $f(\tau,x,\mu)$ is analytic in (x,μ) for $|\mu|$ small. Furthermore, 3) if the real parts of the characteristic roots of matrix D are all negative, then the periodic solution to Eq. (14) is asymptotically stable for $|\mu|$ small. Then, in the steady state, for initial conditions $x|_{\tau=0}$ sufficiently small, all solutions to Eq. (14) approach the periodic solution represented by the method of successive approximations.

Also, for the condition of statement 3 satisfied, statement 1 is also satisfied and it is only necessary to test Eq. (14) with respect to statements 2 and 3.

Since f involves only the first power in x, it is obviously analytic, i.e., representable by a convergent power series, in x. It may be shown that f involves rational functions of b_{13}, b_{23} and $(1 - b_{13}^2 - b_{23}^2)^{1/2}$, all of which are analytic for $|\mu| \ll 1$. Products, quotients and sums of these in f are also analytic since there results no poles (i.e., f bounded) for small $|\mu|$. Consequently, f is analytic and is representable by a convergent power series in (x,μ). Condition 2 is satisfied.

Hurwitz analysis[7] may be used to check condition 3 whether all characteristic roots of matrix D have negative real parts. However, for this case Hurwitz techniques require expansion of determinants of up to order ten. This process may be made manageable by taking advantage of the properties of the two satellite configurations of concern.

For rigid interconnection between satellite sections, C_0 is very large and n_{15} and n_{25} are very much greater than the other n_{ij} of matrix D.

As previously mentioned, a design that attenuates the effect of the motion of B on that of A is desired. Equations (7) and (8) show that the motion of A is decoupled from the motion of B if Ml_Al_B, C_0, C_1 are zero. Although zero values cannot be achieved in practice, this suggests satellite design so that these are small. This low-coupling design is characterized by regarding n_{12}, n_{13}, n_{15}, n_{23}, n_{25} as small compared to the other n_{ij} of matrix D. This corresponds to relatively small gimbal axis torques and to locating the intersection of the gimbal axes close to the mass center of A or B.

† This corresponds to the drive axis aligned along a principal axis of inertia.

The above considerations enable one to neglect higher order powers of small parameters in the expansion of the Hurwitz determinents so that the conditions for all the characteristic roots of matrix D to have negative real parts are that K_0, K_1, K_{03}, K_{13} all be positive for a configuration with rigid interconnection, and that K_0, K_1, K_{03}, K_{13}, C_0, C_1 all be positive for a configuration with low-coupling interconnection.

Consequently, if either of the above conditions is satisfied, the condition of statement 3 is satisfied and for $|\mu|$ and $x|_{\tau=0}$ small, the method of successive approximations may be applied to determine the steady-state solutions of Eq. (14). Carrying terms to first powers in b_{13} and b_{23},

$$\begin{aligned} \phi_1 &= q_{11}s\tau + q_{12}c\tau \quad \phi_2 = q_{12}s\tau - q_{11}c\tau \quad \phi_3 = 0 \\ \theta_1 &= q_{21}s\tau + q_{22}c\tau \quad \theta_2 = q_{22}s\tau - q_{21}c\tau \end{aligned} \tag{18}$$

where

$$\begin{aligned} q_{21} &= [-\lambda_1(V_2 - V_3) + \lambda_2(V_4 - V_1)]/[(V_2 - V_3)^2 + (V_4 - V_1)^2] \\ q_{22} &= [\lambda_1(V_4 - V_1) + \lambda_2(V_2 - V_3)]/[(V_2 - V_3)^2 + (V_4 - V_1)^2] \end{aligned}$$

$$\begin{aligned} \lambda_1 &= 2db_{23} \quad \lambda_2 = 2db_{13} \quad q_{11} = q_{21}N_2 - q_{22}N_1 \\ q_{12} &= q_{21}N_1 + q_{22}N_2 \\ V_1 &= N_2 - U_5 \quad V_2 = N_1 - U_7 \quad V_3 = N_1U_6 \\ V_4 &= U_6(1 + N_2) \\ N_1 &= (U_1U_4 + U_2U_3)/(U_1^2 + U_3^2) \\ N_2 &= (U_3U_4 - U_1U_2)/(U_1^2 + U_3^2) \end{aligned} \tag{19}$$

and

$$\begin{aligned} U_1 &= k_0 - 1 \quad U_2 = -(a + h_{01}) \quad U_3 = k_1 \quad U_4 = h_{11} \\ U_5 &= h_{02} - e_1 \quad U_6 = e_2 \quad U_7 = h_{12} \end{aligned} \tag{20}$$

For small misalignments b_{13}, b_{23} of the drive axis of B, Eq. (18) gives first-order approximations to satellite motion for either rigid interconnection (h_{01}, h_{02} very large) or low-coupling interconnection (h_{01}, h_{02}, h_{11}, h_{12}, and a very small) between A and B [see Eq. (12)].

Discussion of Solution

Rigid Interconnection

For small amplitude motions, the angle ψ_r which the symmetry axis of A makes with its nominal direction (that for which $\phi_1 = \phi_2 = 0$) is accurately given by $\psi_r = (\phi_1^2 + \phi_2^2)^{1/2}$ and taking h_{01} and h_{02} to infinity (representing a per-

fectly rigid interconnection) gives

$$\psi_r = \delta_r/[(1 + R_0)^2 + R_1^2]^{1/2} \tag{21}$$

where

$$\delta_r = (b_{13}^2 + b_{23}^2)^{1/2}|(B_3 - B_1)/(B_3 - J)|$$
$$R_0 = K_0/\omega^2(B_3 - J) \quad R_1 = K_1/\omega(B_3 - J) \tag{22}$$
$$J = J_1 + J_2$$

Since ψ_r is constant with respect to time, the symmetry axis traces a right circular cone with half-angle ψ_r once each period $T = 2\pi/\omega$ sec.

For satellite motion given by the solutions ϕ_1, ϕ_2, ϕ_3, the minimum magnitude $\bar{H}_r$ of CMG angular momentum necessary to provide the control torque of Eq. (1) is determined, as shown in Ref. 4, by integration of the equations of motion for the composite CMG momentum and picking initial conditions to minimize the maximum magnitude of the momentum

$$\bar{H}_r = H_{0r}\{(R_0^2 + R_1^2)/[(1 + R_0)^2 + R_1^2]\}^{1/2} \tag{23}$$

where

$$H_{0r} = (b_{13}^2 + b_{23}^2)^{1/2}\omega|B_3 - B_1| \tag{24}$$

Now the values of ψ_r/δ_r and H_r/H_{0r} can be plotted against R_0 for varying R_1. However, the nature of these curves depends upon whether $B_3 - J$ is greater than or less than zero. Defining $R_0^{\pm} = \pm R_0$, $R_1^{\pm} = \pm R_1$, where the positive sign is taken for $B_3 - J > 0$, and the negative sign is taken for $B_3 - J < 0$, Figure 2 shows the variation of ψ_r/δ_r and $\bar{H}_r/H_{0r}$ with respect to R_0^+ and R_1^+ and Figs. 3 and 4 show the variation of ψ_r/δ_r and $\bar{H}_r/H_{0r}$ with respect to R_0^- and R_1^-. These plots reveal the following: 1) for a satellite with $B_3 - J < 0$, values of K_0 in the region of $K_0 = \omega^2(J - B_3)$ should be avoided. 2) For decreasing R_0^+, R_1^+ or R_0^-, R_1^- corresponding to decreasing CMG spin angular momentum, the satellite coning angle approaches

$$\psi_r = \delta_r = (b_{13}^2 + b_{23}^2)^{1/2}|(B_3 - B_1)/(B_3 - J)| \tag{25}$$

This limiting value of $\psi_r = \delta_r$ is hereafter called the light control coning angle.

For increasing R_0^+, R_1^+ or R_0^-, R_1^-, the control moment gyros cannot have significant effect in decreasing the satellite coning angle until the magnitude of their composite spin angular momentum is of the order of the limiting value

$$\bar{H}_r = H_{0r} = \omega(b_{13}^2 + b_{23}^2)^{1/2}|B_3 - B_1| \tag{26}$$

Low-Coupling Interconnection

For a low-coupling interconnection between bodies A and B, it can likewise be shown that the symmetry axis of A traces a right circular cone with half-angle ψ_l once each period $T = 2\pi/\omega$ sec

$$\psi_l = \delta_l/[(-1 + k_0)^2 + k_1^2]^{1/2} + O_2(h_{01},h_{02},h_{11},h_{12},a) \tag{27}$$

where

$$\delta_l = (b_{13}^2 + b_{23}^2)^{1/2}[(h_{01} + a)^2 + h_{11}^2]^{1/2}|(B_3 - B_1)/\bar{J}|$$
$$\bar{J} = B_3 - B_1 - Ml_B^2 \tag{28}$$

and $O_2(h_{01},h_{02},h_{11},h_{12},a)$ is a term of first order in b_{13} and b_{23} multiplied by second and higher powers of h_{01}, h_{02}, h_{11}, h_{12}, a and consequently may be neglected. Also, dropping higher powers in these small parameters, the minimum magnitude $\bar{H}_l$ of CMG angular momentum necessary to provide the control torques of [Eq. (1)] is determined as shown in Ref. 4.

$$\bar{H}_l = H_{0l}\{(k_0^2 + k_1^2)/[(-1 + k_0)^2 + k_1^2]\}^{1/2} \tag{29}$$

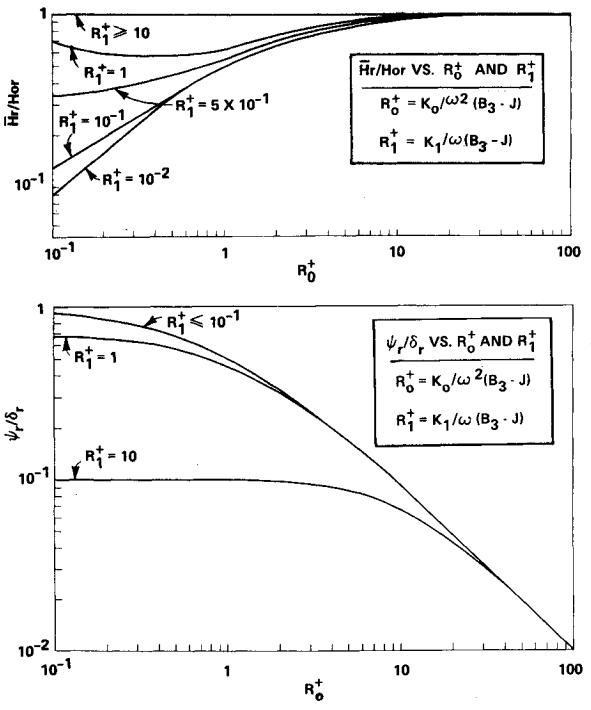

Fig. 2 Coning angle and minimum CMG momentum $B_3 >$ for J.

where

$$H_{0l} = \omega J_1(b_{13}^2 + b_{23}^2)^{1/2}[(h_{01} + a)^2 + h_{11}^2]^{1/2}|(B_3 - B_1)/\bar{J}| \tag{30}$$

The plots of ψ_l/δ_l and $\bar{H}_l/H_{0l}$ are similar to the plots of Figs. 3 and 4 where the ordinates are replaced by ψ_l/δ_l and $\bar{H}_l/H_{0l}$ and R_0^- and R_1^- are replaced by k_0 and k_1, respectively. The following observations may be made: 1) values of K_0 in the region $K_0 = \omega^2 J_1$ should be avoided. 2) The satellite control system is not capable of producing significant reductions in the magnitude of the coning angle from the light control value $\psi_l = \delta_l$ unless the magnitude of the CMG composite angular momentum is at least the

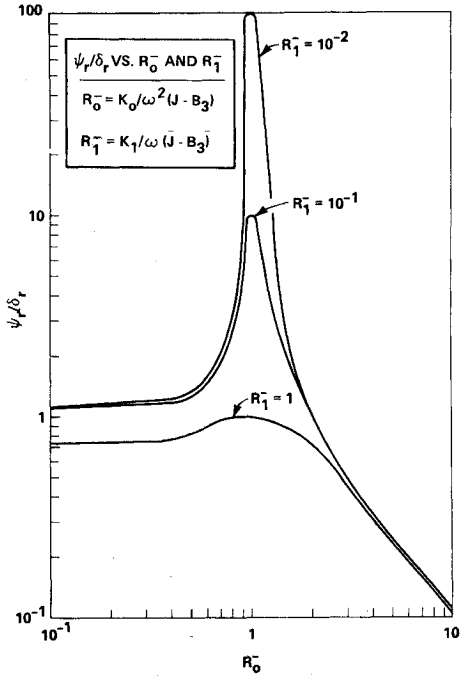

Fig. 3 Coning angle for $B_3 < J$.

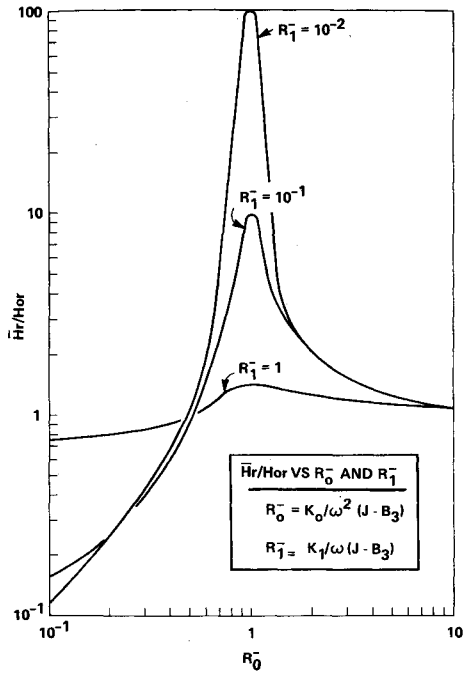

Fig. 4 Minimum CMG momentum for $B_3 < J$.

order of magnitude of the limiting value $\bar{H}_l = H_{0l}$. The assumption that CMGs provide the control torque of Eq. (1) was not used to obtain expressions for the coning angles. Consequently, Eqs. (21) and (27) apply for other types of control.

Applications

Now the coning angle of A and control system requirements for a satellite with a low-coupling interconnection are compared to those for the same satellite with a rigid interconnection. The ratio of light control coning angles is

$$\delta_l/\delta_r = \left|\frac{B_3 - J}{\bar{J}}\right| [(h_{01} + a)^2 + h_{11}^2]^{1/2} \qquad (31)$$

A corresponding ratio of minimum values of CMG composite angular momentum necessary to significantly reduce the light control coning angles is

$$H_{0l}/H_{0r} = [(h_{01} + a)^2 + h_{11}^2]^{1/2} J_1/\bar{J} \qquad (32)$$

Consequently, for h_{01}, a, h_{11} small quantities corresponding to small gimbal axes torque coefficients and the gimbal axes intersection located near the mass center of A or B, both the magnitude of the light control coning angle and control system requirements necessary to reduce that angle can be substantially smaller for a low-coupling interconnection between the spinning and despun bodies than for a rigid interconnection.

This can be further illustrated by example. NASA has suggested for study[8] a large space base that consists of a hub with a nonrotating section, and a rotating section to which three spokes are attached in a Y fashion and which is spinning so as to provide an artificial gravity compartment at the extremities of one of the spokes. To within NASA's margin of error for mass estimates, the space base is assumed to be axially symmetrical with the following mass properties: $B_3 = 9.5 \times 10^8$ slug-ft^2; $M_A = 1.1 \times 10^4$ slugs; $l_A + l_B = 17$ ft; $M_B = 3.1 \times 10^4$ slugs. Additional data was not available. However, the spinning section B presents a flat profile and its inertia characteristics approach those of a plane figure. Hence, the following appears reasonable

$$B_1 = 4.85 \times 10^8 \text{ slug/ft}^2$$

and

$$A_1 = 3.2 \times 10^7 \text{ slug/ft}^2$$

Now due to uncertainties in construction, structural deformations, and relocations of men and equipment, misalignment of 0.5° and more of the spinning section principal axis of inertia from the spin axis appears possible.

By Eq. (25), a 0.5° misalignment results in a light-control coning angle of $\psi_r = \delta_r = 0.54°$. A coning angle of 0.54° is likely unacceptable. This amplitude of motion is outside the fine pointing requirements for many experiments planned for future space stations.[9] Also, for this amplitude and $\omega = 4$ rpm, locations at distances greater than four feet from the space base mass center experience instantaneous accelerations greater than 10^{-4} g. Some experiments, such as those involving crystal growth, require accelerations perhaps less than 10^{-5}g.

Now if for these or other reasons the coning angle is unacceptable, then, as declared in the aforementioned statement 2 for a significant reduction the CMGs must have a momentum capacity of at least the order of H_{0r}. For $\omega = 4$ rpm, Eq. (26) gives $\bar{H}_r = H_{0r} = 1.69 \times 10^6$ ft-lb-sec, a value far beyond the capacity of existing CMGs, 2300 ft-lb-sec CMG for the Skylab type.

Now for the same configuration designed with a low-coupling interconnection, the parameter a can be made less than 4×10^{-3} by constructing the gimbal system such that the gimbal axes intersection lies one foot or less from the mass center of either body. Also, even for gimbal axes torques of the order of 1000 ft lb, h_{01} and h_{11} are less than 0.05.

Consequently, taking $a = 4 \times 10^{-3}$, $h_{01} = h_{11} = 0.05$, $l_B = 1$ ft and using Eq. (31), $\delta_l = 0.068 \times \delta_r = 0.037°$. Also, for a significant reduction in this coning angle, the CMGs must have a momentum capacity of at least the order of H_{0l}. From Eq. (32), $H_{0l} = 0.537 \times 10^{-2} \times H_{0r} = 9100$ ft-lb-sec, a value which could be provided by four Skylab CMGs.

In practice values of h_{01} and h_{11} much less than 0.05 probably can be obtained. Although these potentially offer greater reductions in motion and control requirements, such small h_{01} and h_{11} are not considered here due to mathematical complications resulting from these quantities approaching the size of the measure $|\mu|$ of spin axis misalignment. Questions of stability arise because it is necessary to consider h_{01} and h_{11} as being of the order of $|\mu|$ so that terms involving these are shifted from matrix D to matrix F in Eq. (14). Then D has zero characteristic roots and the foregoing stability analysis does not apply.

Nevertheless, it seems probable that stability difficulties do not occur except for imaginary parts of the characteristics roots for matrix D of Eq. (14) in the regions of $2n\pi$, $n = \pm 1, \pm 2, \ldots$; and for system design to avoid these regions, very small values of h_{01} and h_{11} and corresponding very small motions and control requirements could be achieved. However, to verify this supposition requires more general techniques, the most practical probably being numerical Floquet analysis. Since the main purpose of this study is to demonstrate that low-coupling interconnection may offer advantages over rigid interconnection, such a detailed computerized approach requiring specific choices of system parameters is beyond the scope of this work.

Finally, criteria other than stability and isolation could affect the selection of h_{01} and h_{11} and other system parameters. One example is time for transients to decay.

Appendix A: Periodic Solutions to a Set of Differential Equations

Coddington and Levinson[6] have set forth sufficient conditions for existence and asymptotic stability of periodic solu-

tions to a set of differential equations of the form

$$x' = f(\tau,x,\mu) \tag{A1}$$

where x is a column vector with n components, f is periodic in τ of period T, and μ may be a real constant vector. In addition, a method of successive approximations is established for determining these periodic solutions.

Following is a brief outline of the discussions of Ref. 6 with a slight modification in the statement of the method of successive approximations allowing μ to be a column vector with two components rather than a scalar.

For each τ, let f be analytic (i.e., each f_i, $i = 1, \ldots, n$ is representable by a convergent power series) in (x,μ) for $|\mu|$ small, and consider the case where Eq. (A1) with $\mu = 0$ has a solution p of period T. Defining the first variation of Eq. (A1)

$$y' = \sum_{j=1}^{n} \frac{\partial f}{\partial x_j}(\tau,p(\tau),0)y_j = f_x(\tau,p(\tau),0)y \tag{A2}$$

then,

Theorem 1

If Equation (A2) has no solution of period T other than the trivial solution $y = 0$, then for small $|\mu|$, Eq. (A-1) has a unique solution $q = q(\tau,\mu)$ periodic in τ of period T with $q(\tau,0) = p(\tau)$.

Also, it may be shown that q is analytic in μ for small $|\mu|$ and any τ. Then, $q(\mu,\tau)$ has a convergent power series representation, which for μ a column vector with dimension two

$$\mu = \begin{bmatrix} \mu_1 \\ \mu_2 \end{bmatrix}$$

has the form

$$q(\tau,\mu) = p^{(0)}(\tau) + \mu_1 p^{(1,1)}(\tau) + \mu_2 p^{(1,2)}(\tau) + \ldots \tag{A3}$$

Also, by assumption $f(\tau,q(\tau,\mu),\mu)$ has a power series representation and substituting this together with Eq. (A3) into Eq. (A1) and equating powers of μ_1, μ_2, there results

$$dp/d\tau_{(\tau)}{}^{(0)} = f[\tau,p^0(\tau),0]$$

$$dp^{(1,1)}/d\tau_{(\tau)} = f_x[\tau,p^{(0)}(\tau),0]p_{(\tau)}{}^{(1,1)} + \partial f[\tau,p^{(0)}(\tau),0]/\partial\mu_1 \tag{A4}$$

$$dp^{(1,2)}/d\tau_{(\tau)} = f_x[\tau,p^{(0)}(\tau),0]p_{(\tau)}{}^{(1,2)} + \partial f[\tau,p^{(0)}(\tau),0]/\partial\mu_2$$

where $p^{(0)}(\tau) = p(\tau)$. Since q is known to exist as an analytic function of μ, the system (A4) provides that solution. Sufficient conditions for stability of q follow.

Theorem 2

If the real parts of the characteristic exponents of Eq. (A2) are negative, then the solution $q = q(\tau,\mu)$ of Eq. (A1) is asymptotically stable provided $|\mu|$ and $|x|_{\tau=0}$ are small.

References

[1] Pringle, R. Jr., "Stability of the Force-Free Motions of a Dual Spin Spacecraft," *AIAA Journal*, Vol. 7, No. 6, June 1969, pp. 1054–1063.

[2] Proceedings of the Symposium on Attitude Stabilization and Control of Dual Spin Spacecraft, TR-0158(3307-01)-16, Nov. 1967, Aerospace Corp., El Segundo, Calif.

[3] Likins, P. W., "Attitude Stability Criteria for Dual-Spin Spacecraft," *Journal of Spacecraft and Rockets*, Vol. 4, No. 12, Dec. 1967, pp. 1638–1643.

[4] Wenglarz, R. A., "Problems in Attitude Control of Artificial 'G' Space Stations with Mass Unbalance," *Journal of Spacecraft and Rockets*, Vol. 7, No. 10, Oct. 1970, pp. 1161–1166.

[5] Cretcher, C. K. and Mingori, D. L., "Nutation Damping and Vibration Isolation in a Flexibly Coupled Dual-Spin Spacecraft," *Journal of Spacecraft and Rockets*, Vol. 9, No. 8, Aug. 1971, pp. 817–823.

[6] Coddington, E. A. and Levinson, N., *Theory of Ordinary Differential Equations*, McGraw-Hill, New York, 1955, pp. 348–351.

[7] Wilts, C. H., *Principles of Feedback Control*, Addison-Wesley, Reading, Mass., 1960, pp. 63–64.

[8] "Space Station, Phase B Study," 1969, NASA, p. A-14.

[9] Kurzhals, P. R., "T-013 Objectives and Application," July 1963, NASA.